BBA - Molecular Basis of Disease 1865 (2019) 464–475

Contents lists available at ScienceDirect

BBA - Molecular Basis of Disease

journal homepage: www.elsevier.com/locate/bbadis

Oxidized hemoglobin forms contribute to NLRP3 inflammasome-driven IL-1β production upon intravascular hemolysis

Benard Bogonko Nyakundi[a,1], Andrea Tóth[a,1], Enikő Balogh[a], Béla Nagy[b], Judit Erdei[a], Bernhard Ryffel[c,d], György Paragh[a], Mario D. Cordero[e], Viktória Jeney[a,*]

[a] Research Centre for Molecular Medicine, Faculty of Medicine, University of Debrecen, Debrecen, Hungary
[b] Department of Laboratory Medicine, Faculty of Medicine, University of Debrecen, Debrecen, Hungary
[c] Experimental and Molecular Immunology and Neurogenetics, The National Center for Scientific Research, Orleans, France
[d] Institute of Molecular Medicine, University of Cape Town, Cape Town, South Africa
[e] Institute of Nutrition and Food Technology "José Mataix Verdú", Department of Physiology, Biomedical Research Center, University of Granada, Granada, Spain

ARTICLE INFO

Keywords:
Hemolysis
Ferryl hemoglobin
Heme
NLRP3 inflammasome activation
IL-1β
Macrophage

ABSTRACT

Damage associated molecular patterns (DAMPs) are released form red blood cells (RBCs) during intravascular hemolysis (IVH). Extracellular heme, with its pro-oxidant, pro-inflammatory and cytotoxic effects, is sensed by innate immune cells through pattern recognition receptors such as toll-like receptor 4 and nucleotide-binding domain and leucine rich repeat containing family, pyrin domain containing 3 (NLRP3), while free availability of heme is strictly controlled. Here we investigated the involvement of different hemoglobin (Hb) forms in hemolysis-associated inflammatory responses.

We found that after IVH most of the extracellular heme molecules are localized in oxidized Hb forms. IVH was associated with caspase-1 activation and formation of mature IL-1β in plasma and in the liver of C57BL/6 mice. We showed that ferrylHb (FHb) induces active IL-1β production in LPS-primed macrophages *in vitro* and triggered intraperitoneal recruitment of neutrophils and monocytes, caspase-1 activation and active IL-1β formation in the liver of C57BL/6 mice. NLRP3 deficiency provided a survival advantage upon IVH, without influencing the extent of RBC lysis or the accumulation of oxidized Hb forms. However, both hemolysis-induced and FHb-induced pro-inflammatory responses were largely attenuated in *Nlrp3*$^{-/-}$ mice.

Taken together, FHb is a potent trigger of NLRP3 activation and production of IL-1β *in vitro* and *in vivo*, suggesting that FHb may contribute to hemolysis-induced inflammation. Identification of RBC-derived DAMPs might allow us to develop new therapeutic approaches for hemolytic diseases.

1. Introduction

Sterile hemolysis is associated with inflammation mainly due to the release of damage associated molecular patterns (DAMPs) during red blood cell (RBC) destruction [1,2]. Hemoglobin (Hb) composes 96% of the dry weight of RBCs that is protected from oxidation by the highly efficient antioxidant network inside the RBCs [3]. On the other hand once outside of the protective environment of RBCs, Hb is prone to oxidation, leading to the formation of oxidized Hb forms, *i.e.* metHb (MHb) and ferrylHb (FHb) [3–9]. Oxidation of the heme iron weakens the association between heme and the globin chain therefore oxidized Hb forms are able to release heme. An endogenous protective system controls the harmful effects of extracellular Hb and heme. This relies mainly on the presence of Hb- and heme-binding proteins in the plasma, particularly haptoglobin (Hp) and hemopexin (Hx) which facilitate clearance of extracellular Hb and heme from the circulation *via* receptor mediated endocytosis [10–13]. This protective system can be overwhelmed upon massive intravascular hemolysis leading to the accumulation of Hb and heme in the plasma [10–13].

Accumulating evidence reveals that free heme exerts both pro-oxidant [14–17] and pro-inflammatory actions [3,18,19]. As a pro-inflammatory molecule, heme induces tumor necrosis factor alpha (TNFα) secretion *via* a Toll like receptor 4 (TLR4)-dependent mechanism in macrophages [20], TLR4-dependent degranulation of Weibel-Palade bodies and nuclear factor κB (NF-κB) activation in endothelial cells [21], and triggers neutrophil extracellular trap formation

* Corresponding author.
E-mail address: viktoria.jeney@med.unideb.hu (V. Jeney).
[1] The first two authors equally contributed to these studies.

https://doi.org/10.1016/j.bbadis.2018.10.030
Received 27 July 2018; Received in revised form 16 October 2018; Accepted 26 October 2018
Available online 30 October 2018

as well [22]. Additionally, free heme induces Nucleotide binding domain, Leucine rich Repeat containing Protein 3 (NLRP3) inflammasome activation, and subsequent production of interleukin 1 beta (IL-1β) in both macrophages and endothelial cells [23,24]. Furthermore, recently it has been shown that cell-free heme and heme-loaded microvesicles formed upon intravascular hemolysis activates the complement system [25,26]. This mechanism can contribute to thrombosis and organ injury in hemolytic uremic syndrome and sickle cell disease [25,26].

Recent evidence shows that heme scavenging by Hx cannot attenuate renal dysfunction in an experimental model of intravascular hemolysis, suggesting that besides free heme, other components released upon RBC destruction play a pathophysiological role in these conditions. In line of this notion, extracellular Hb and oxidized Hb forms has been reported to exhibit diverse pro-inflammatory actions [27]. For example, cell-free Hb impairs nitric oxide (NO) bioavailability and that NO replacement partially prevents acute hemolysis-induced inflammatory processes [28]. Importantly, FHb is a strong pro-inflammatory agonist that triggers NF-κB activation in endothelial cells leading to increased expression of cellular adhesion molecules and disruption of the endothelial monolayer integrity, independently of heme release [29]. Moreover, oxidized forms of Hb, *i.e.* MHb and FHb are known pro-oxidants which actions are considered to be dependent on heme release from these species [17,30,31].

Heme is a prototypical alarmin, involved in hemolysis-induced lethality *via* triggering NLRP3 activation in macrophages, but we lack knowledge whether extracellular Hb or oxidized Hb forms could contribute to inflammation triggered by sterile hemolysis. Therefore, we investigated the involvement of different Hb forms to NLRP3 inflammasome activation and subsequent production of IL-1β in a mice model of sterile hemolysis.

2. Materials and methods

2.1. Materials

Reagents were purchased from Sigma-Aldrich (St. Louis, MO, USA) unless otherwise specified.

2.2. Animals

C57BL/6 (wild type, WT) and *Nlrp3*$^{-/-}$ mice on a C57BL/6 background were maintained at the University of Debrecen in a conventional animal house. The *Nlrp3*$^{-/-}$ mice strain was originally generated and characterized in the laboratory of J. Tschopp [32]. In the experiments we used age- and sex-matched male and female mice between 6 and 8 weeks of age. All experiments were carried out in accordance with the principles of the Basel Declaration and followed guidelines of the institutional and national ethical committee and underwent approval (Approval registration number: 2/2016/DEMÁB, issued by the University of Debrecen, Committee of Animal Welfare). Mice were euthanized by CO_2 inhalation, and blood was drawn by heart puncture into heparinized tubes. Plasma samples were obtained by centrifugation of blood at 2000 × *g*, 15 min, 4 °C. Livers and spleens were collected after perfusion of the mice with 5 mL of sterile ice-cold PBS.

2.3. Hemolysis protocol and mouse treatments

Hemolysis was induced in mice by intraperitoneal (i.p.) administration of phenylhydrazine (PHZ). PHZ was applied twice, first 50 mg/kg body weight and 16 h later 30 mg/kg body weight. In time course experiments mice were sacrificed 4 or 16 h after the first dose of PHZ, or 4 h after the second PHZ injection (20 h). In some experiments we injected the mice with heme, Hb, MHb and FHb at a dose of 300 nmol heme group, or with LPS 100 μg/peritoneal cavity in a volume of 200 μL. Control mice received 200 μL apyrogen PBS in all experiments and in some experiments we applied controls without treatment as well.

2.4. Hematocrit (Hct) measurement

K_3-EDTA anticoagulated murine whole blood samples were analyzed by Siemens Advia-2120i hematology analyzer (Tarrytown, NY, USA) with 800 Mouse C57BL program of Multi Species software. Hct values were determined as a calculated parameter derived from RBC count (RBC in T/L) and mean cell volume (MCV in fL). The number of RBCs was multiplied by the MCV of the sample RBCs and was divided by 1000.

2.5. Hb preparation

Hb of different redox states, *i.e.* Hb (Fe^{2+}), MHb (Fe^{3+}), and FHb (Fe^{4+} = O), were prepared as described [29]. Briefly, Hb was isolated from fresh blood drawn from healthy volunteers using ion-exchange chromatography on a DEAE Sepharose CL-6B column. MHb was generated by incubation (30 min, 25 °C) of purified Hb with a 1.5-fold molar excess of $K_3Fe(CN)_6$ over heme. FHb was obtained by incubation (1 h, 37 °C) of Hb with a 10:1 ratio of H_2O_2 to heme. The ferryl state of iron is highly unstable therefore FHb is transiently forms. During stabilization of ferryl iron different chemically heterogeneous oxidized Hb molecules are formed which we refer as FHb to reflect rather the way of their formation than their actual oxidation status. After oxidation, both MHb and FHb were dialyzed against saline (3 times for 3 h at 4 °C) and concentrated using Amicon Ultra centrifugal filter tubes (10,000 MWCO, Millipore Corp., Billerica, MA, USA). Aliquots were snap-frozen in liquid nitrogen, and stored at −70 °C until use. Endotoxin content of Hb preparations was analyzed by Limulus amebocyte lysate assay (Lonza, Walkersville, MD, USA). Purity of each Hb preparation was evaluated by SDS-PAGE followed by staining with ProteoSilver Plus Silver Staining Kit. The purity of Hb preparations was above 99.9%. Molar concentrations for all Hb solutions used throughout this paper are based on heme.

2.6. Determination of Hb concentrations at different oxidation status

Optical densities at 541, 560, 576 and 630 nm were determined with a Hewlett Packard HP 8453 spectrophotometer. To calculate Hb and MHb concentrations the recently reported equations and extinction coefficients were used [33]. Hemichrome concentrations were calculated as described previously [4].

2.7. Determination of plasma total heme concentration and calculation of non Hb-bound heme

Plasma total heme content was determined with QuantiChrom Heme Assay Kit (BioAssay Systems, Hayward, CA, USA) following the manufacturer's instructions. This kit measures the sum of bioavailable and protein-bound heme. Non Hb-bound heme concentration was calculated with the use of the following equation: [non Hb-bound heme] = [total heme] − [Hb] − [MHb] − [hemichrome].

2.8. Cell culture and treatments

Murine RAW 264.7 macrophage cell line was purchased from ATCC (Manassas, VA, USA). Cells were cultured in DMEM supplemented with 10% heat inactivated fetal bovine serum (Gibco, Waltham, MA, USA), L-glutamine and 1% penicillin/streptomycin in 5% CO_2 humidified atmosphere at 37 °C. When indicated RAW cells were pretreated with 10 ng/mL LPS (0111: B4 from *Escherichia coli*) for 4 h. Bone marrow macrophages (BMMs) were isolated using tibia and femur from 8 to 12 weeks old C57BL/6 mice. Bone marrow was obtained by flushing the opened bones with 10 mL of complete DMEM. Bone marrow cells were counted, re-suspended in complete medium supplemented with 50 ng/mL M-CSF (Miltenyi Biotec, Bergisch Gladbach, Germany), and seeded at a density of 3 × 10^5 cell/well in 96-well tissue culture plates. After

7 days of culture, non-adherent cells were removed and adherent cells were used in the experiments. When indicated, BMMs were pretreated with 10 ng/mL LPS in complete DMEM containing 10% heat inactivated FBS for 4 h. Heme and Hb treatments of both cell types (RAW and BMMs) were carried out in DMEM supplemented with 1% heat inactivated FBS.

2.9. Quantitative real-time PCR (qRT-PCR)

RNA was isolated from cells using TRIzol (RNA-STAT60, Tel-Test Inc., Friendswood, TX, USA) according to the manufacturer's protocol. Two micrograms of RNA were reverse transcribed to cDNA with High-Capacity cDNA Reverse Transcription Kit (Applied Biosystems, Waltham, MA, USA). Quantitative RT-PCR was performed using iTaq Universal Probes Supermix (Bio-Rad Laboratories, Hercules, CA, USA) and predesigned primers and probes (TaqMan® Gene Expression Assays) to detect IL-1β (Mm 00434228), HO-1 (Mm 00516005) and GAPDH (Mm 99999915). Relative mRNA expressions were calculated with the ΔΔCt method using GAPDH as internal control.

2.10. Western blot

Liver lysates were used to investigate caspase-1 activation and IL-1β processing. Protein samples (20 μg) were run on 12.5% SDS-PAGE. Western Blotting was performed with the use of a polyclonal anti-caspase-1 p20 antibody (sc-398,715, Santa Cruz Biotechnology Inc., Dallas, TX, USA), and a monoclonal anti-IL-1β antibody (12,242, Cell Signaling Technology, Leiden, The Netherlands). HO-1 expression was evaluated from liver and whole cell lysate (20 μg) with the use of a polyclonal HO-1 antibody (ADI-SPA-896, Enzo Life Sciences Inc., Farmingdale, NY, USA). HRP-conjugated anti-rabbit and anti-mouse antibodies were used as secondary antibodies (NA931 and NA934, Amersham Biosciences Corp., Piscataway, NJ, USA). Antigen-antibody complexes were visualized with the horseradish peroxidase chemiluminescence system (Amersham Biosciences Corp., Piscataway, NJ, USA). After detection, the membranes were stripped and reprobed for β-actin using HRP-conjugated anti-β-actin antibody (sc-47778, Santa Cruz Biotechnology Inc., Dallas, TX, USA). Hb was detected with the use of a HRP-conjugated polyclonal anti-Hb antibody (ab-19362, Abcam, Cambridge, UK). Results were quantified by using Alpha DigiDoc RT (Alpha Innotech, San Leandro, CA, USA) quantification system.

2.11. IL-1β secretion in macrophages

Following treatments cellular supernatants were collected and 100 μL of undiluted sample was used for ELISA analysis (DuoSet ELISA, R&D, Minneapolis, MN). All of the measurements were performed according to the manufacturer's protocol.

2.12. Determination of cell viability

Cell viability was determined by the MTT assay as previously described [17]. Briefly, following treatments, cells were washed with PBS, and 100 μL of 3-[4,5-Dimethylthiazol-2-yl]-2,5-diphenyl-tetrazolium bromide (0.5 mg/mL dissolved in HBSS) solution was added. After a 4-h incubation the MTT solution was removed, formazan crystals were dissolved in 100 μL of DMSO and optical density was measured at 570 nm.

2.13. Intracellular ROS measurement

ROS production was monitored by using the 5-(and-6)-chloromethyl-2′,7′-dichlorodihydro-fluorescein di-acetate, acetyl ester (CM-H_2DCFDA) assay (Life Technologies, Carlsbad, CA, USA). After the treatment cells were washed with PBS and loaded with CM-H_2DCFDA (10 μmol/L, 30 min, in the dark). After loading the cells with CM-H_2DCFDA, cells were washed thoroughly with PBS and fluorescence intensity was monitored for 3 h applying 488 nm excitation and 533 nm emission wavelengths.

2.14. Mouse peritonitis model

Twenty-five WT mice (male and female, 8–10 weeks of age) were randomly divided into 5 groups ($n = 5$/group) and injected i.p. with heme and Hb forms at a dose of 300 nmol heme group/peritoneal cavity in 200 μL apyrogen PBS. Control mice received PBS only. After 16 h, mice were sacrificed by CO_2 exposure and peritoneal leukocytes were harvested by peritoneal lavage using ice-cold PBS containing 2% FCS (Gibco, Waltham, MA, USA) and were analyzed by flow cytometry. Total number of cells was determined using a fixed number of latex beads (Beckman Coulter, Paris, France), co-acquired with a pre-established volume of the cell suspensions. Number of peritoneal neutrophils was evaluated using R-phycoerythrin (R-PE)-conjugated rat anti-mouse Ly-6G (Gr1; CD11b, BD Biosciences, San Jose, CA) and biotin anti-mouse neutrophil monoclonal antibody (Clone 7/4, CL8993B, Cedarlane, Hornby, Ontario, Canada). Cells were co-stained with propidium iodide (0.5 μg/mL) to exclude dead cells. Fluorescence was measured by flow cytometry (FACS Calibur, BD Biosciences) and data was analyzed using FlowJo software (Tree Star, Inc. Ashland, OR). Ly-6G and 7/4 double positive cells were identified as neutrophils, Ly-6G negative, 7/4 positive cells were considered as inflammatory monocytes/macrophages [34].

2.15. Statistical analysis

Data are shown as mean ± S.D. Statistical analysis was performed by one-way ANOVA or Student's *t*-test, as appropriate. $P < 0.05$ was considered significant.

3. Results

3.1. Intravascular hemolysis (IVH) is associated with the formation of Hb forms with different oxidation status

Following RBC lysis, Hb outside of the protective environment of RBCs tends to be oxidized. Because oxidation of Hb is a complex process and can lead to the formation of different oxidized Hb species, first we wanted to determine the plasma concentrations of Hb forms following IVH in mice. To trigger IVH we injected PHZ (50 mg/kg body weight and 30 mg/kg body weight 16 h later) into the peritoneal cavity of WT mice whereas control mice received PBS (Fig. 1A). A well-known effect of severe IVH is splenomegaly, therefore to monitor the condition, we collected spleen and blood samples at 4 h, 16 h (before the second injection), and at 20 h time points. PHZ injection triggered marked enlargement of the spleen at 20 h post-injection and yellowish/brownish discoloration of the plasma at every time points (Fig. 1A). A single PHZ injection induced a substantial decrease in hematocrit levels at 4 h time point compared to PBS-injected controls (0.5 ± 0.01 *v*/v% *vs.* 0.36 ± 0.05 v/v%) (Fig. 1B). Hematocrit levels further decreased to 0.31 ± 0.01 v/v% after the second PHZ injection (Fig. 1B). Next we determined plasma total heme levels. A single injection of PHZ triggered a robust elevation in plasma total heme levels as compared to PBS-injected controls at 4 h post-injection (18.4 ± 1.6 μmol/L *vs.* 80.5 ± 16.9 μmol/L) (Fig. 1C). The second PHZ injection further increased total plasma heme level up to 123.6 ± 16.4 μmol/L (Fig. 1C). Then we determined Hb, metHb and hemichrome levels in the plasma samples of PHZ-injected mice (Fig. 1D–F). Naïve Hb levels were elevated in plasma samples collected from PHZ-injected mice at 16 h and 20 h time points (Fig. 1D). Interestingly, 4 h after PHZ injection most of the heme was in the form of oxidized Hbs, particularly hemichrome (52.84 ± 6.9 μmol/L) and metHb (30.07 ± 6.44 μmol/L) (Fig. 1E and

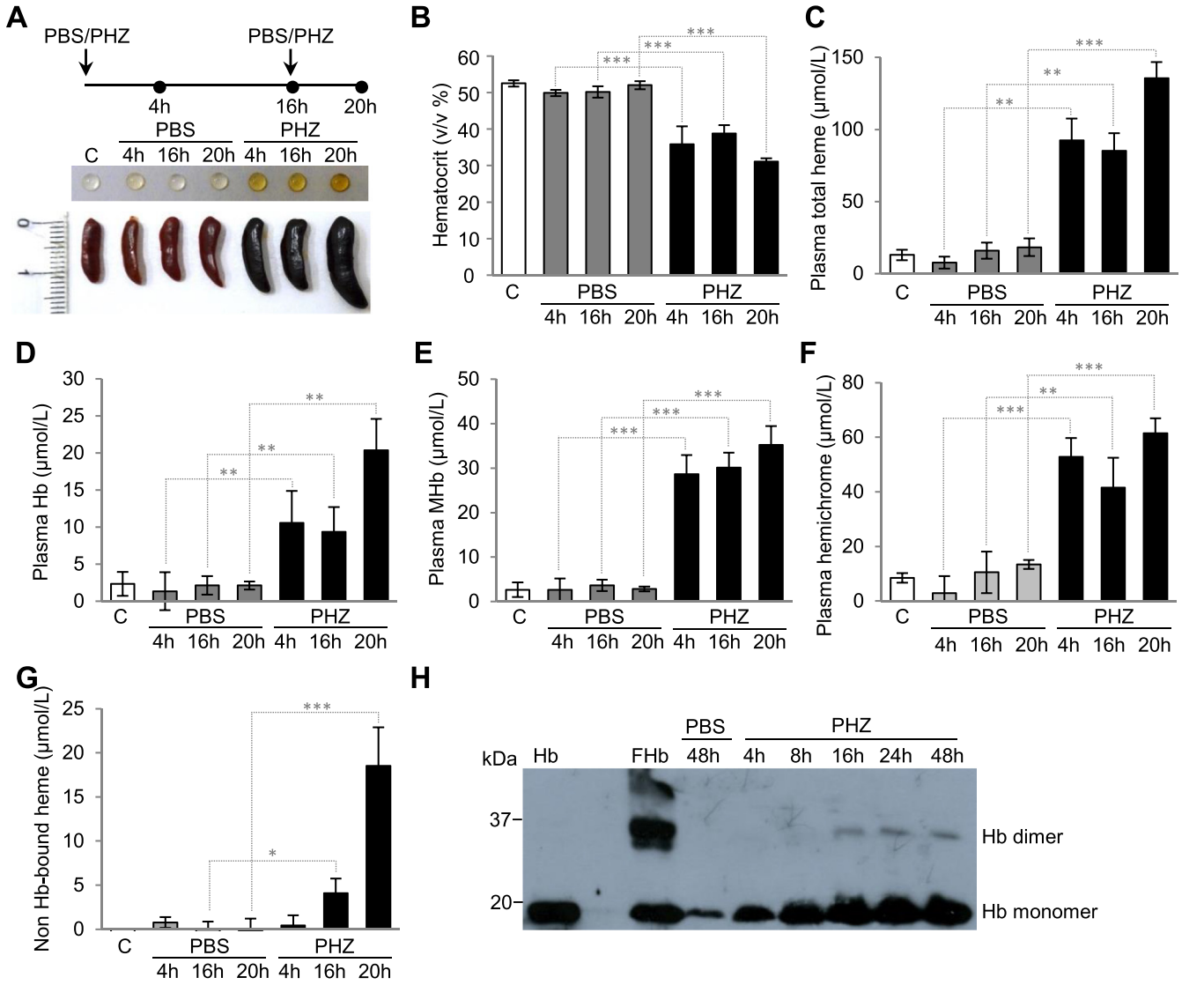

Fig. 1. Intravascular hemolysis induces accumulation of Hb, oxidized Hb forms and free heme in the plasma.
(A–H) C57BL/6 mice were injected (i.p.) with PHZ (50 mg/kg, then 30 mg/kg mice at 16 h, $n = 5$) or PBS (n = 5) or left untreated (C), n = 5). Mice were sacrificed and samples were collected at 4, 16 and 20 h time points. (A) Schedule of the experiment. Representative images of plasma discoloration and spleen enlargement upon PHZ treatment are shown. (B) Hematocrit, (C) plasma total heme, (D) plasma Hb, (E) plasma MHb, (F) plasma hemichrome, (G) plasma free heme levels are shown as mean ± SD. *$P < 0.05$. **$P < 0.01$. ***$P < 0.005$. (H) Representative Hb western blot of plasma samples taken at the indicated time points. As controls we show purified human hemoglobin (Hb) and oxidized Hb (FHb).

F). At this time point we could detect very low levels of non-Hb bound heme (1.05 ± 0.56 μmol/L) that we refer "free heme" here (Fig. 1G). Similarly, majority of heme was present in oxidized Hb forms in plasma samples taken 16 and 20 h after PHZ injection (Fig. 1D–F). Free heme level started to increase in plasma of PHZ-injected mice 16 h post-injection (1.2 ± 2.36 μmol/L *vs.* 5.9 ± 4.15 μmol/L) and became markedly elevated in plasma of PHZ-treated mice compared to PBS-injected controls at 20 h time point (32.67 ± 1.13 μmol/L *vs.* 0.85 ± 1.23 μmol/L) (Fig. 1D-G). Extensive oxidation of Hb leads to the formation of ferryl and oxyferryl Hb species, those instable intermediates that decay *via* intramolecular electron transfer giving a rise to the formation of globin radicals. Termination of globin radicals leads to the formation of covalently crosslinked Hb forms with potential pro-inflammatory effects. Therefore, we wanted to investigate whether these covalently cross-linked Hb forms are present in the plasma following intravascular hemolysis. We found that Hb dimers were present in plasma samples obtained from PHZ-injected mice but not in the plasma of PBS-injected control mice (Fig. 1H).

3.2. IVH is associated with processing of IL-1β and caspase-1 activation

Dutra el al showed that heme induces NLRP3 activation and IL-1β production in macrophages, and that this mechanism contributes to hemolysis-induced lethality in mice [23]. To further examine this phenomenon, we measured plasma levels of IL-1β in PHZ-injected WT mice. In agreement with the previous observation of Dutra et al. PHZ-induced hemolysis was associated with elevation of IL-1β plasma concentrations at 16 h and 20 h time points (Fig. 2A). The liver is largely responsible for free hemoglobin uptake following intravascular hemolysis, therefore next we analyzed livers of PHZ-injected mice [35]. We observed dark discoloration but no other obvious changes in the livers of PHZ-injected mice compared to PBS-injected mice (Fig. 2B). Expression of heme oxygenase-1 (HO-1), the enzyme responsible for cellular degradation of heme, was markedly elevated (10.39 ± 1.36-fold increase *vs.* vehicle control) in the liver of PHZ-treated mice analyzed at 20 h post-injection (Fig. 3C). Furthermore, we detected increased levels of cleaved IL-1β in liver samples obtained from PHZ-injected WT mice

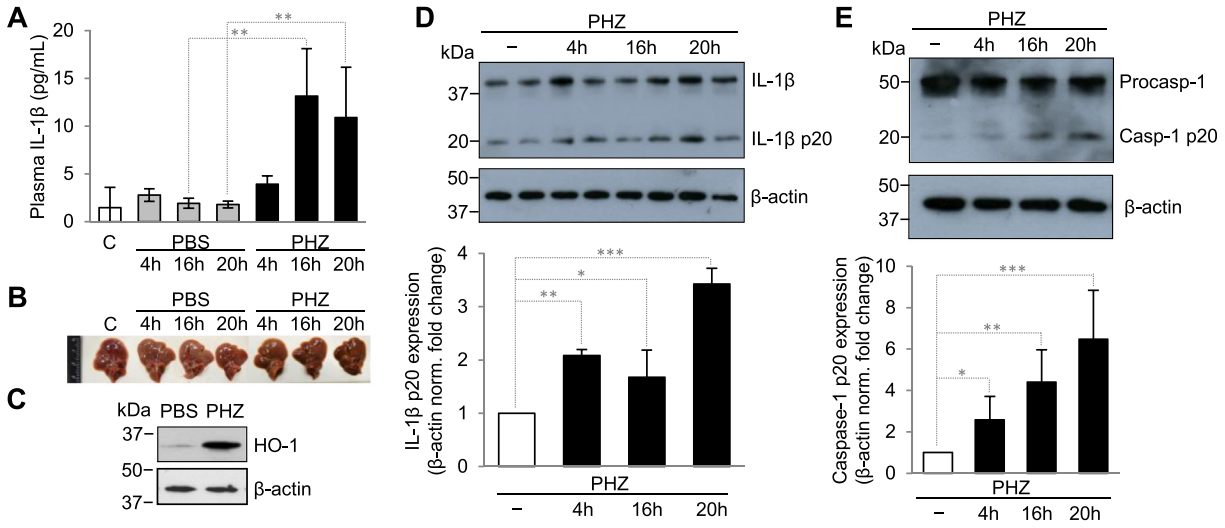

Fig. 2. Intravascular hemolysis triggers IL-1β production and caspase-1 activation.
(A–D) C57BL/6 mice were injected (i.p.) with PHZ (50 mg/kg, then 30 mg/kg mice at 16 h, n = 5) or PBS (n = 5) or left untreated (C), n = 5). Mice were sacrificed and samples were collected at 4, 16 and 20 h time points. (A) IL-1β levels from plasma were determined by ELISA and are shown as mean ± SD. (B) Representative images of liver upon PHZ treatment and controls are shown.(C-D) Protein expressions of processed IL-1β (IL-1β p20) and activated caspase-1 (Casp-1 p20) were analyzed by Western blot from liver samples at indicated time points. Membranes were reprobed for β-actin. Representative blots of 3 independent experiments are shown. Densitometric analysis of Western blots is shown as mean ± SD of 3 independent experiments. $^{*}P < 0.05$. $^{**}P < 0.01$. $^{***}P < 0.005$.

at all time points (Fig. 2C), that was associated with time-dependent activation of caspase-1, suggesting NLRP3 inflammasome activation (Fig. 2D).

3.3. FHb but not naïve Hb or MHb induce IL-1β processing in macrophages

Previous studies showed that heme induces IL-1β production in macrophages, suggesting that free heme plays a central role in hemolysis-associated formation of IL-1β [23]. Distribution of plasma heme following IVH revealed that most of the plasma heme is localized in oxidized Hb forms, and that elevation of IL-1β levels in the plasma of PHZ-injected mice (Fig. 2A) precedes the accumulation of non Hb-bound heme (Fig. 1G). Therefore, we hypothesized that other Hb forms produced after intravascular hemolysis contribute to the formation of IL-1β. To address this question first we purified Hb from human blood of healthy donors and used to generate Hb forms with different oxidation status MHb and FHb. We obtained characteristic absorption spectra for each Hb forms (Fig. 3A). Purity of the Hb preparations was higher than 95%, as assessed by silver staining after SDS/PAGE separation (Fig. 3B). Silver staining (Fig. 3B) and Western blotting (Fig. 3C) revealed that Hb and MHb were present as 16 kDa monomer subunits. In contrast we detected covalently crosslinked Hb multimers in FHb preparation (Fig. 3B and C) which is consistent with previous reports [29]. Then we treated LPS-primed RAW264.7 murine macrophages with heme (25 μmol/L) as a positive control, and Hb forms with different oxidation status, Hb, MHb and FHb (25–150 μmol/L). In agreement with the previously published results of Dutra et al. [23] heme induced a marked upregulation of IL-1β mRNA in LPS-primed RAW macrophages that was associated with increased processing and secretion of IL-1β (Fig. 4A and B). Among the Hb forms naïve Hb and MHb induced IL-1β mRNA, but failed to increase the level of processed IL-1β in cellular supernatants (Fig. 4A and B). In contrast, FHb caused marked upregulation of IL-1β mRNA and increased processing and secretion of IL-1β (Fig. 4A and B). Next, we examined the effect of Hb forms on IL-1β secretion in LPS-primed BMMs. Similarly to that of RAW macrophages only heme and FHb induced IL-1β processing and secretion in BMMs (Fig. 4C). LPS priming was necessary to trigger heme of FHb-induced IL-1β production in both RAW cells and BMMs as non-primed cells failed to respond to heme or FHb stimulation (data not shown).

3.4. Pro-inflammatory actions of Hb forms

Next, we examined whether Hb forms with different oxidation status exerts pro-inflammatory actions *in vivo* when injected into the peritoneal cavity of WT mice. We found that heme and FHb induced marked intraperitoneal infiltration of neutrophils and monocytes in WT mice (Fig. 5A–C). In contrast, naïve Hb did not induce peritoneal infiltration of leukocytes, while MHb triggered only a mild increase in the number of peritoneal neutrophils but did not induced monocyte

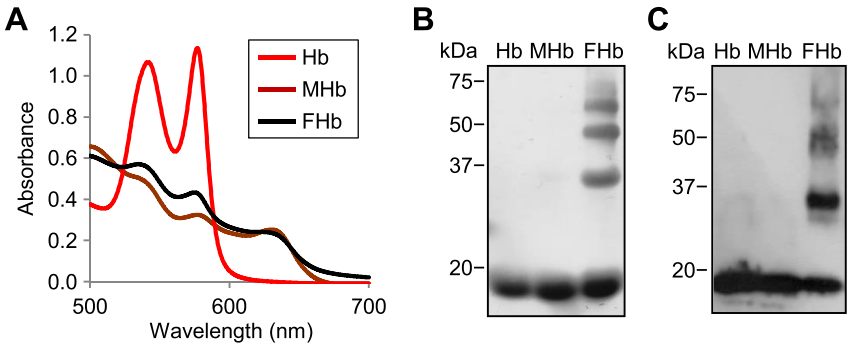

Fig. 3. Characterization of purified Hb, MHb, and FHb solutions.
(A) Absorbance spectra of purified Hb, MHb and FHb solutions at the concentrations of 60 μmol/L. (B) Representative silver staining ($N = 3$) following SDS-PAGE of Hb, MtHb, and ferrylHb (5 nmol/lane). (C) Representative western blot ($N = 5$) of Hb, mHb and FHb (5 nmol/lane).

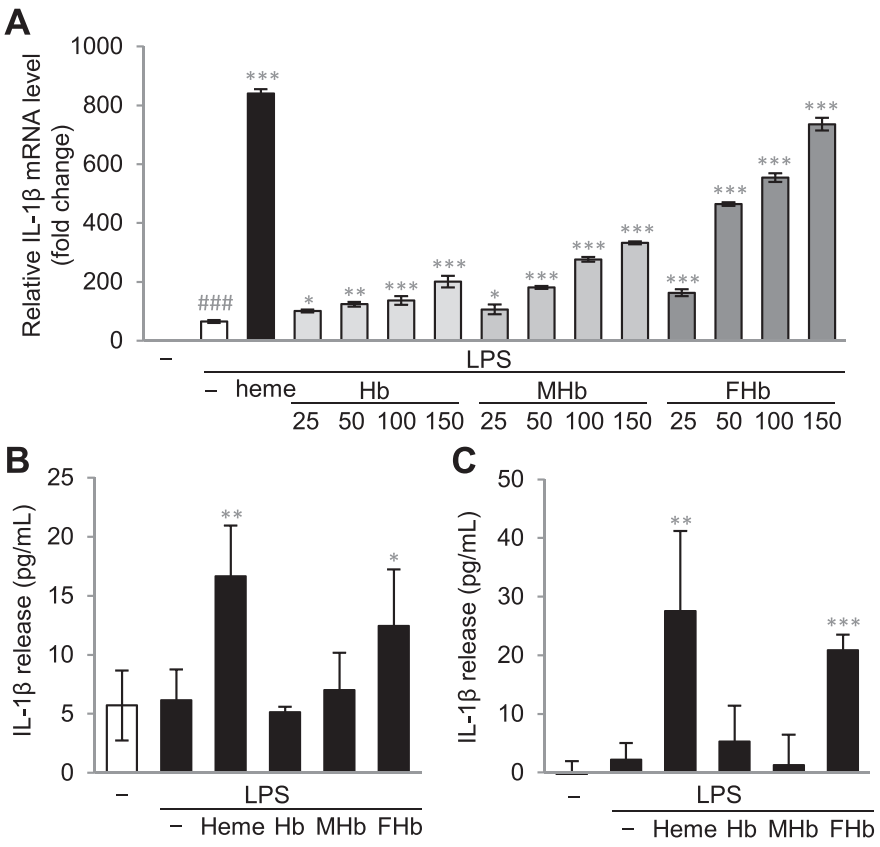

Fig. 4. Induction of IL-1β production by free heme and Hb forms in macrophages.
(A) LPS primed (10 μg/mL, 24 h) RAW cells were exposed to heme (25 μmol/L) or different Hb forms (Hb, MHb or FHb) at a concentration of 25, 50, 100, 150 μmol/L in DMEM containing 1% FBS for 4 h. IL-1β mRNA levels were determined by qRT-PCR. (B) LPS primed (10 μg/mL, 24 h) or non-primed RAW cells were exposed to heme (25 μmol/L) Hb, MHb or FHb (150 μmol/L in DMEM containing 1% FBS, 6 h). IL-1β levels from cellular supernatant were determined by ELISA. (C) LPS primed (10 μg/mL, 24 h) or non-primed BMMs were exposed to heme (25 μmol/L) Hb, MHb or FHb (150 μmol/L in DMEM containing 1% FBS, 6 h). IL-1β levels from cellular supernatant were determined by ELISA. Results are shown as mean ± SD from 3 independent experiments performed in triplicates. $^{*}P < 0.05$. $^{**}P < 0.01$. $^{***}P < 0.005$.

recruitment (Fig. 5A–C). In our previous experiment, we showed that PHZ-induced hemolysis was associated with caspase-1 activation and IL-1β processing in the liver therefore next we investigated the effect of different Hb forms in inflammasome activation in the liver of WT mice. Intraperitoneal administration of all the Hb forms as well as heme induced caspase-1 activation in the liver of WT mice (Fig. 5D). Among the different Hb forms the most potent inducer of caspase-1 activation was FHb that induced an 8-fold increase in the expression of cleaved caspase-1 (Fig. 5D). Parallel with caspase-1 activation, we observed marked elevation of processed IL-1β in the liver of FHb as well as heme-treated WT mice (Fig. 5E). In comparison to FHb and heme, Hb and MHb were much less potent agonists to induce IL-1β processing in livers of WT mice (Fig. 5E).

3.5. Deficiency of NLRP3 provides tolerance to mice against intravascular hemolysis-mediated lethality

Massive intravascular hemolysis can be lethal. In our PHZ-induced hemolysis model 75% of WT mice succumbed 2 to 6 days after the first PHZ injection. In contrast, only 33% of PHZ-injected NLRP3 deficient mice died within the same period (Fig. 6A). The mice survived the first 7 days following the first PHZ treatment recovered and lived up to 10 days when we terminated the experiment (Fig. 6A). To see whether PHZ treatment results the same extent of hemolysis in WT and *Nlrp3*$^{-/-}$ mice, first we compared hematocrit levels following PHZ injections. We found no difference between hematocrit levels of PHZ-treated WT and NLRP3 deficient mice (Fig. 6B). Then we compared the levels of extracellular Hb forms in plasma of WT and NLRP3 mice following PHZ injections. We found similar levels of Hb, MHb and hemichrome in plasma samples obtained from WT and *Nlrp3*$^{-/-}$ mice (Fig. 6D–E). These results suggest that NLRP3 deficient mice are more tolerant to PHZ-induced hemolysis and extracellular Hb forms than WT mice.

3.6. NLRP3 is essential to both hemolysis-triggered and FHb-induced inflammation

IVH triggers IL-1β processing in the liver. To investigate whether NLRP3 is involved in hemolysis-induced production of IL-1β, we treated WT and NLRP3 deficient mice with PHZ and assessed IL-1β levels in the liver. PHZ treatment induced marked elevation of cleaved IL-1β in WT mice livers, whereas we did not observe increased IL-1β processing in the livers of PHZ-treated *Nlrp3*$^{-/-}$ mice (Fig. 7A). Next, we investigated the involvement of NLRP3 in FHb-induced processing of IL-1β using WT and *Nlrp3*$^{-/-}$ mice. We injected WT and *Nlrp3*$^{-/-}$ mice with vehicle, FHb and LPS that served as a positive control. We found increased levels of processed IL-1β in the livers of both LPS and FHb-treated WT mice in comparison to vehicle-injected controls. In contrast, we observed no increase in IL-1β processing in livers of either LPS- or FHb-treated *Nlrp3*$^{-/-}$ mice compared to vehicle-treated controls (Fig. 7B). These results suggest that NLRP3 is essential to the production of active IL-1β in response to hemolysis or FHb.

3.7. Hb-mediated IL-1β production is associated with heme uptake and ROS production in macrophages

Macrophages take up heme in different forms and are considered to be the major cell types involved in heme-iron recycling. Following uptake, heme is released and degraded by the inducible enzyme HO-1. To see whether the different Hb forms could serve as heme sources towards macrophages we determined HO-1 mRNA and protein expressions in RAW macrophages treated with different Hb forms. Heme is the strongest inducer of HO-1 in macrophages, and caused a > 30-fold elevation in HO-1 mRNA level at the dose of 25 μmol/L (Fig. 8A). Our results revealed that among the Hb forms, FHb is the most potent Hb form in inducing HO-1 mRNA and protein expressions in RAW macrophages (Fig. 8B and C). Heme uptake of macrophages is associated with elevated production of ROS formation (Fig. 8D). Among the

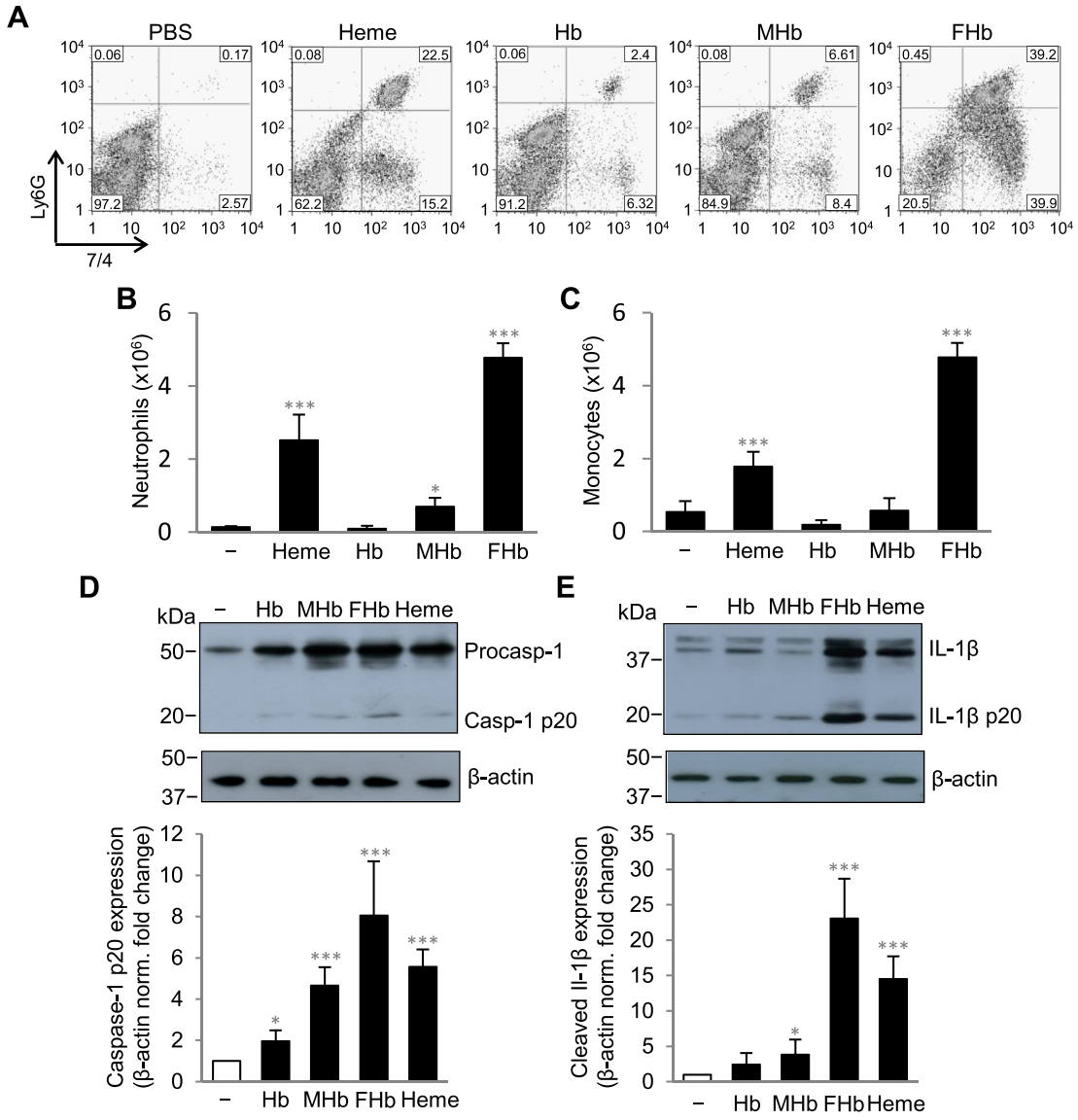

Fig. 5. Induction of peritonitis, liver caspase-1 activation and IL-1β processing by free heme and Hb forms in mice.
(A–E) C57BL/6 mice were injected (i.p.) with heme or Hb forms (300 nmol heme/mice, n = 5/each group) or PBS (n = 5). (A–C) Peritoneal cavity was rinsed, neutrophil and inflammatory monocytes/macrophage numbers were determined after 16 h of treatment. (A) Representative dot plots of peritoneal cells stained with Ly-6G and 7/4. (B) Mean number of Ly-6G high and 7/4 high PMN cells. (C) Mean number of Ly-6G low, 7/4 high inflammatory monocytes/macrophages. Data are presented as mean ± SD. (D-E) Protein expressions of activated caspase-1 (Casp-1 p20) and processed IL-1β (IL-1β p20) were analyzed by Western blot from liver samples. Membranes were reprobed for β-actin. Representative blots of 3 independent experiments are shown. Densitometric analysis of Western blots is shown as mean ± SD of 3 independent experiments. $*P < 0.05$. $**P < 0.01$. $***P < 0.005$.

Hb forms naïve Hb and MHb did not increase ROS production in macrophages even when we applied at higher doses. In contrast, FHb induced ROS formation in a dose-dependent manner (Fig. 8E). Heme-mediated unfettered ROS production in macrophages was associated with decreased cell viability. In contrast, none of the Hb forms triggered cell death of RAW macrophages (Fig. 8F).

4. Discussion

In this study, we report the contribution of different Hb forms produced upon IVH to NLRP3 inflammasome activation and subsequent production of IL-1β with the use of *in vitro* approaches and a mice model of sterile hemolysis. We show that besides heme, oxidized Hb forms, in particular FHb contribute to the production of the pro-inflammatory cytokine IL-1β. We also show the critical involvement of NLRP3 in FHb-mediated formation of IL-1β.

While Hb is compartmentalized in RBCs its extensive oxidation is prevented by a highly effective antioxidant defense system including enzymatic (Cu/Zn superoxide dismutase, catalase, glutathione peroxidase, and peroxiredoxins) as well as non-enzymatic (glutathione) scavengers [3,36,37]. Furthermore auto-oxidation of Hb into MHb is controlled by MHb reductase. Outside of the protective environment of RBCs, Hb is prone to oxidation.

Auto-oxidation of Hb leads to the formation of MHb and superoxide anions. Two-electron oxidation of Hb is triggered by peroxides, *e.g.* H_2O_2, leading to the formation of FHb. The reaction of MHb with H_2O_2 yields FHb radical ($Hb\cdot^{+}(Fe^{4+} = O^{2-})$) in which the unpaired electron is associated with the globin or the porphyrin ring [5–8]. Because these Hb forms contain high-valence iron, they are highly reactive that can decay by several routes [38]. Iron can be stabilized *via* an intramolecular electron transfer between the ferryl iron and specific amino acid residues such as αTyr-24, αTyr-42, αHis-20, βTyr-35, βTyr-

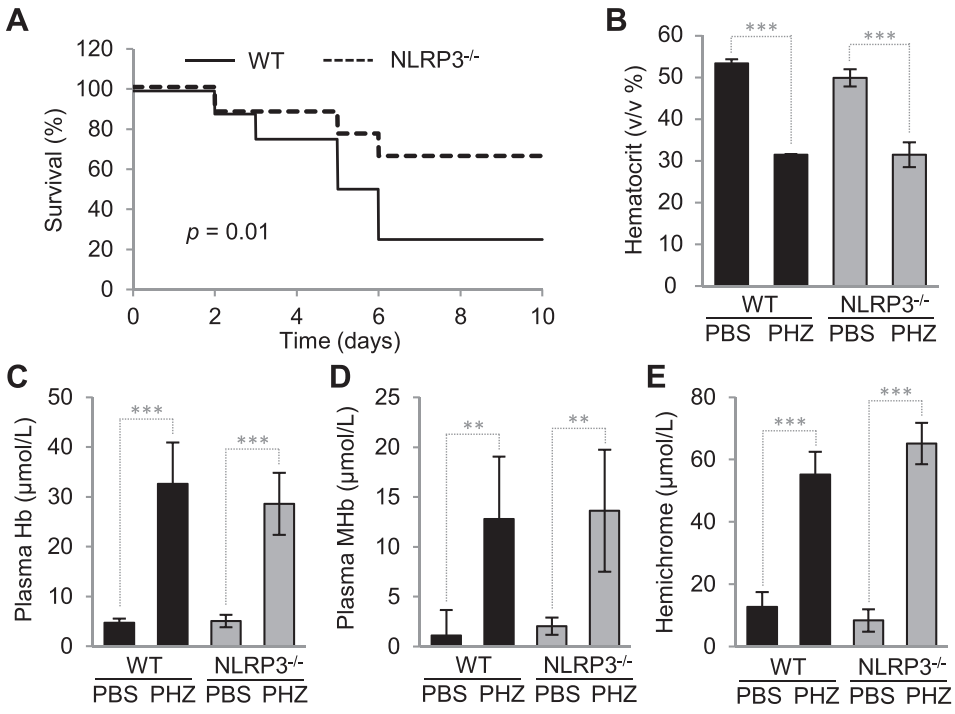

Fig. 6. Deficiency of NLRP3 provides tolerance to mice against intravascular hemolysis-mediated lethality.
(A) C57BL/6 mice and *Nlrp3*$^{-/-}$ mice were injected (i.p.) with PHZ (50 mg/kg, then 30 mg/kg mice at 16 h, $n = 11$/group). Survival of mice was monitored for 10 days. (B-E) C57BL/6 mice and *Nlrp3*$^{-/-}$ mice were injected (i.p.) with PHZ (50 mg/kg, then 30 mg/kg mice at 16 h, n = 5/group) or PBS (n = 5). Mice were sacrificed and plasma samples were collected at 20 h time point. Hematocrit (B), Hb (C), MHb (D) and hemichrome (E) levels were determined by spectral analysis of the plasma samples. Data is presented as mean ± SD of 3 independent experiments. $^{*}P < 0.05$. $^{**}P < 0.01$. $^{***}P < 0.005$.

130, and βCys-93 of the globin chains resulting in the formation of MHb globin radical [3,39,40]. Furthermore, termination reactions between globin- and porphyrin-centered radicals give a rise to globin-globin and porphyrin-globin adducts.

Here we used a well-established model of acute sterile hemolysis to investigate the formation of these Hb species *in vivo*. In agreement with previous observations, acute intravascular hemolysis induced marked splenomegaly and decreased hematocrit levels in C57BL/6 mice (Fig. 1A and B) [41]. Parallel with the hematocrit we assessed plasma heme level by Heme Assay Kit. We revealed profound elevation of extracellular heme concentrations up to ~130 μmol/L (Fig. 1C), which is very similar to the previously reported plasma total heme levels in PHZ-injected mice measured by formic acid method [42]. More detailed examination of plasma heme content revealed that most of the heme moiety can be found in hemichrome, a denatured form of oxidized Hb. Dominance of hemichromes among the produced Hb species upon intravascular hemolysis may be attributed to the use of PHZ which is a very strong oxidant [43]. A lesser amount of heme was present in Hb and metHb, and at 20 h post-injection we calculated that about 20 μmol/L heme was dissociated from the hemoglobins (Fig. 1D–G). The amount of bioavailable heme in the plasma of PHZ-injected mice was measured recently with a novel approach using heme-specific single domain antibodies and a cellular-based heme reporter assay [42]. They reported that the amount of bioavailable heme is around 2–5 μmol/L [42]. Therefore we assume that most of the non Hb-bound heme we detected with our assay is associated with specific and non-specific heme-binding proteins or transferred to hydrophobic lipid compartments [17,44,45].

Besides hemichromes, Hb, metHb and non Hb-bound heme we could identify covalently crosslinked Hb dimers in plasma samples of PHZ-injected mice, which is an indirect evidence of the formation of the highly reactive ferryl species (Fig. 1H).

RBC-derived microparticles (RMPs) are heme-loaded small phospholipid vesicles shed from RBCs. There is growing evidence that these RMPs are bioactive particles and contribute to the pathogenesis of sickle cell disease and RBC storage lesions [25,46–49]. We applied low speed centrifugation of blood to obtain plasma samples therefore RMPs could influence the determination of plasma Hb and heme levels in this study.

Abundant evidence indicates that extracellular Hb and free heme are harmful, explaining the evolvement of efficient mechanisms that control their deleterious effects. The plasma acute phase proteins Hp and Hx are in the first line of defense upon intravascular hemolysis. Hp captures cell free Hb and facilitates its clearance through the CD163 macrophage scavenger receptor-mediated endocytosis [10,11]. Besides this function, Hp binding protects Hb from oxidation, because Hb residues known to be prone to oxidative modifications are buried in the Hp:Hb interface [50–55]. Hx sequesters free heme with the highest affinity of any known proteins in an inert, non-toxic form [12]. Following capture, Hx-heme complexes are internalized *via* the scavenger receptor LDL receptor-related protein 1/CD91 mainly by hepatocytes and macrophages [13,56]. The protective effects and the therapeutic potential of Hp and Hx have been elucidated in various hemolytic models (reviewed in [57,58]).

In case of massive intravascular hemolysis both Hp and Hx are consumed, leading to the accumulation cell-free Hb, oxidized Hb forms and free heme that we have observed in our acute hemolysis model (Fig. 1). Accumulating evidence suggests that extracellular Hb, oxidized Hb forms and free heme possess specific pro-inflammatory activities. For example, FHb impairs endothelial barrier function through upregulation of adhesion molecules and formation of intercellular gaps [29]. Several studies suggest pro-inflammatory actions of free heme *via* the activation of pattern recognition receptors such as TLR4 or NLRP3 in leukocytes and endothelial cells [20–24,59–62].

Based on our results PHZ-induced intravascular hemolysis is associated with increased plasma concentration of IL-1β. Additionally, our results revealed that intravascular hemolysis induces caspase-1 activation and the formation of active IL-1β in the liver (Fig. 2). The involvement of liver is well-known in free hemoglobin clearance following intravascular hemolysis [63]. Both hepatocytes [35] and Kupffer cells can internalize extracellular hemoglobin [64] and both cell types respond to cellular danger signals by activating caspase-1 and releasing the pro-inflammatory cytokines IL-1β and IL-18 [65]. Further studies are needed to identify the nature of IL-1β producing cells in the liver.

Previous work of Dutra et al. revealed that heme triggers production of IL-1β in macrophages which contributes to hemolysis-associated lethality. Interestingly, we found that the increase in IL-1β plasma

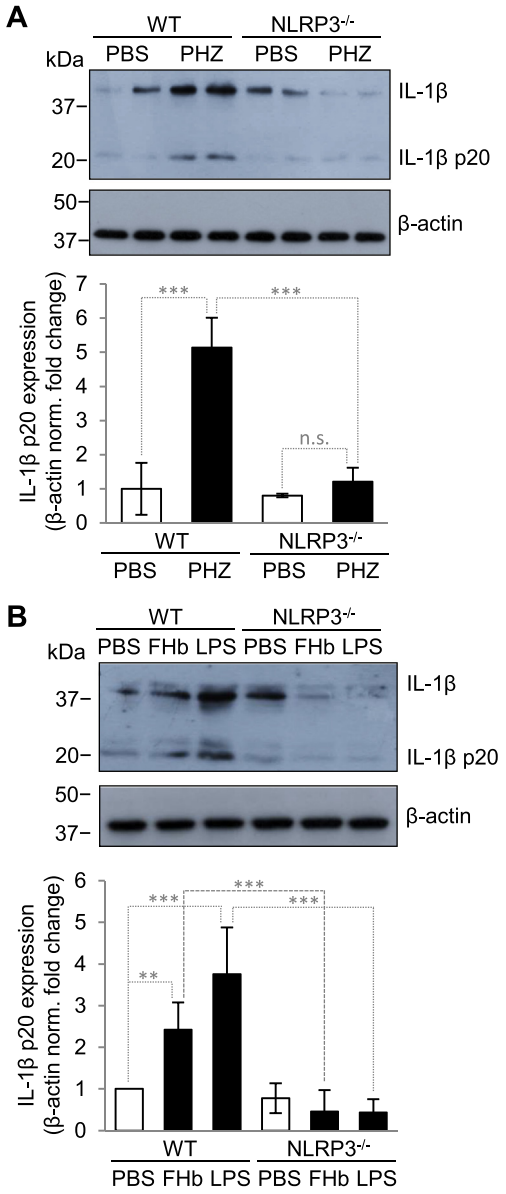

Fig. 7. NLRP3 is essential to hemolysis-associated IL-1β processing.
(A) C57BL/6 mice and *Nlrp3*$^{-/-}$ mice were injected (i.p.) with PHZ (50 mg/kg, then 30 mg/kg mice at 16 h, n = 5/group) or PBS (n = 5). (B) C57BL/6 mice and *Nlrp3*$^{-/-}$ mice were injected (i.p.) with PBS, FHb (300 nmol heme/peritoneal cavity), or LPS (100 μg/peritoneal cavity). (A–B) Mice were sacrificed and liver samples were collected at 20 h time point. Protein expression of processed IL-1β (IL-1β p20) was analyzed by Western blot from liver samples. Membranes were reprobed for β-actin. Representative blots of 3 independent experiments are shown. Densitometric analysis of Western blots is shown as mean ± SD of 3 independent experiments. *$P < 0.05$. **$P < 0.01$. ***$P < 0.005$.

levels precedes the accumulation of non-Hb bound heme in the plasma (Figs. 1 and 2), therefore we tested the different Hb forms upstream of free heme whether they are involved in the inflammatory response triggered by intravascular hemolysis.

When exposed *in vitro* to FHb, LPS-primed macrophages markedly up-regulate IL-1β mRNA (Fig. 4A). To a lesser extent, both Hb and MHb increase the level of IL-1β mRNA (Fig. 4A). Similarly to that of heme, FHb is able to induce processing of IL-1β in macrophages (Fig. 4B and C). On the contrary, naïve Hb and MHb lack the ability to induce IL-1β secretion *in vitro* (Fig. 4B and C).

LPS priming was necessary to induce IL-1β production in heme or FHb-treated macrophages. This is in agreement with the widely accepted mechanism of inflammasome activation that requires two distinct signals [66]. In contrast, PHZ injection without LPS treatment was enough to trigger IL-1β production in the liver in our *in vivo* model. We speculate that gut-derived LPS could serve as a first signal in the induction of IL-1β as it was confirmed previously in an experimental model of alcoholic liver disease [67,68]. This potential mechanism needs to be confirmed in PHZ-induced intravascular hemolysis model by further studies. *In vivo* administration of FHb through intraperitoneal injection provokes peritonitis, characterized by massive infiltration of neutrophils and monocytes into the peritoneal cavity (Fig. 5A–C). Heme, to a lesser extent, also induces neutrophil and monocyte recruitment. In contrast, injection of naïve Hb does not trigger leukocyte infiltration, and MHb provokes only minor neutrophil recruitment (Fig. 5A–C). This result is in agreement with previously published results of Silva et al., in which the authors showed that FHb induces peritoneal recruitment of neutrophils [29]. As a response to intravascular hemolysis caspase-1 is activated and IL-1β is processed in the liver (Fig. 2), therefore we used this approach to further investigate the pro-inflammatory role of different Hb forms. Intraperitoneal administration of FHb and heme induced caspase-1 activation and processing of IL-1β (Fig. 5D and E).

Activation of different innate immune receptors including NLRP1, NLRP3, NLRC4 or AIM2 could lead to maturation and secretion of active IL-1β through the assembly of the inflammasome and activation of inflammatory caspases [69–72]. Among these immune receptors, the critical role of NLRP3 inflammasome complex was established previously in heme-mediated IL-1β production in macrophages as well as in endothelial cells [23,24,73]. Dutra et al. showed that survival rates of mice lacking NLRP3 inflammasome components such as NLRP3, apoptosis-associated speck-like protein containing a caspase activation and recruitment domain (ASC) or Caspase-1 are remarkable higher than WT mice upon intravascular hemolysis [23]. To further investigate this phenomenon first we confirmed the survival advantage NLRP3 deficient mice in our acute PHZ-induced hemolysis model (Fig. 6A). Theoretically survival advantage of these knock-out mice strains can rely on their increased resistance to PHZ-induced RBC lysis, or their increased tolerance to lysis. Measurement of hematocrit levels of WT and *Nlrp3*$^{-/-}$ mice subjected to PHZ-induced hemolysis revealed that NLRP3 deficiency does not impair RBC lysis therefore this mechanism cannot explain increased survival rate of *Nlrp3*$^{-/-}$ mice compared to WT (Fig. 6B). Moreover, we found no difference between plasma concentrations of Hb, MHb or hemichrome in WT and *Nlrp3*$^{-/-}$ mice (Fig. 6C–E), suggesting that NLRP3 deficient mice has increased tolerance to lysis.

Tissue damage control in response to infection as well as sterile inflammation can improve survival of the host in diverse disease conditions [74]. In response to hemolysis NLRP3 inflammasome is activated leading to the production of the pro-inflammatory cytokine IL-1β in the liver of WT mice. In contrast, there is no active IL-1β production in the liver of PHZ-, or FHb-treated *Nlrp3*$^{-/-}$ mice (Fig. 7A and B). Lack of the pro-inflammatory response in NLRP3 deficient mice might contribute to the improved survival of those mice under hemolytic conditions.

We demonstrated that the extensively oxidized Hb form, FHb is as potent trigger as heme of NLRP3 inflammasome activation under both *in vitro* and *in vivo* conditions. It is well established that oxidized Hb forms, *i.e.* MHb and FHb are able to release heme, because oxidation of the heme iron weakens the association between heme and the globin chain. Based on this feature, MHb and FHb exhibit pro-oxidant activities supported by the notion that they induce oxidative modification of low-density lipoprotein (LDL) similarly to that of free heme [17,31]. Moreover, heme released by oxidized Hb forms can be taken up by diverse cells including endothelial cells and amplify oxidant-mediated killing [16,30]. Macrophages internalize both heme and naïve Hb through receptor mediated endocytotic pathways and catabolize heme

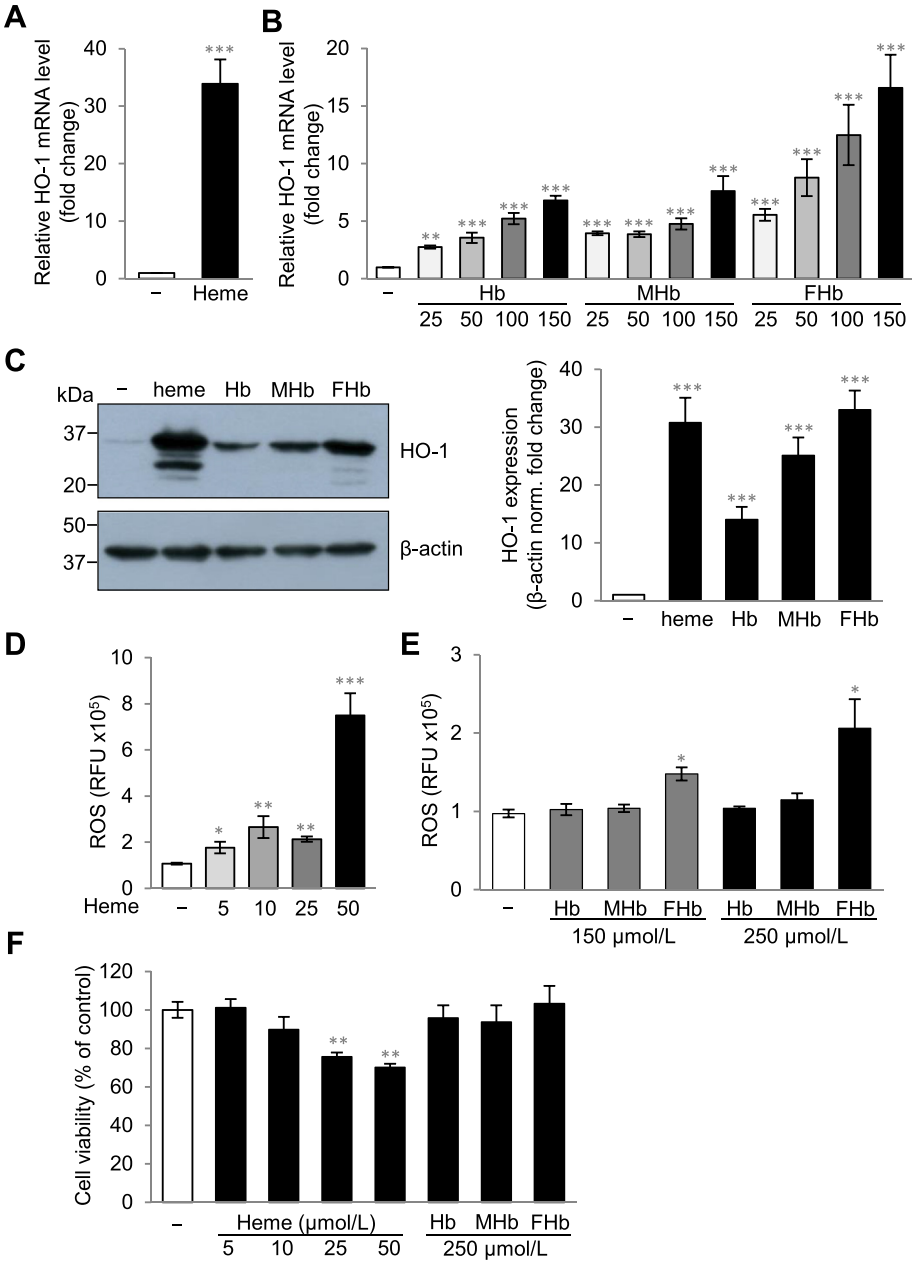

Fig. 8. Hb-mediated IL-1β production is associated with heme uptake and ROS production in macrophages.
RAW cells were exposed to (A) heme (25 µmol/L) or (B) different Hb forms (Hb, MHb or FHb) at a concentration of 25, 50, 100, 150 µmol/L in DMEM containing 1% FBS for 4 h hours. HO-1 mRNA levels were determined by qRT-PCR. Results are shown as mean ± SD from three experiments performed in triplicates. (C) RAW cells were treated with heme (25 µmol/L) or different Hb forms (150 µmol/L) for 8 h. Protein expression of HO-1 was evaluated by Western blot. Membranes were reprobed for β-actin. Representative blots of 3 independent experiments are shown. Densitometric analysis of Western blots is shown as mean ± SD of 3 independent experiments. (D–E) RAW cells were exposed to heme (0–50 µmol/L) or different Hb forms (Hb, MHb or FHb) at a concentration of 150 and 250 µmol/L in DMEM containing 1% FBS for 4 h. Following the treatment ROS production was measured with DCFDA assay. (F) RAW cells were exposed to heme (0–50 µmol/L) or different Hb forms (Hb, MHb or FHb) at a concentration of 250 µmol/L in DMEM containing 1% FBS for 8 h. Following the 8-h treatment cell viability was measured with MTT assay. (D–F) Data is presented as mean ± SD of 3 independent experiments performed in quadruplicates. $^{*}P < 0.05$. $^{**}P < 0.01$. $^{***}P < 0.005$.

via the action of heme oxygenases (HO). Heme exposure triggers marked upregulation of HO-1. Our results revealed that besides free heme Hb forms with different oxidation states upregulated HO-1 mRNA and protein expressions, suggesting the Hb forms served as a heme source for macrophages (Fig. 8A–C). Interestingly, we found that FHb is more potent in inducing HO-1 in RAW macrophages than naïve Hb or MHb (Fig. 8B and C). In a recent work heme release from various hemoglobin redox states was studied using heme scavenger proteins and lung epithelial cells as reporter systems [75]. This study showed undoubtedly that MHb releases heme at a faster rate, and triggers higher HO-1 expression in lung epithelial cells than FHb [75]. The difference between the two observations may reflect that the release and subsequent uptake of heme might not be the exclusive mechanism of obtaining heme from various Hb forms in macrophages. Comparing to free heme, all Hb forms including FHb are much weaker inducers of HO-1 suggesting that heme uptake and/or heme release from oxidized Hb forms is incomplete. This is in agreement with previous findings showing that MHb and FHb cause delayed oxidative modification of LDL due to lower numbers of LDL-associated heme groups compared to free heme [17,31].

NLRP3 inflammasome activation is triggered by several structurally diverse molecules that share some common molecular mechanisms through which inflammasome activation occurs, including elevated ROS production, K^+ efflux, lysosomal damage as well as ATP release [76–79]. Dutra et al. showed that ROS production plays a critical role in heme-mediated NLRP3 inflammasome activation and IL-1β production. We confirmed that heme induces ROS production in macrophages (Fig. 8D). Evaluation of ROS production in macrophages treated with different Hb forms revealed that FHb increases ROS formation although to a lesser extent compared to heme (Fig. 8D and E). On the contrary, naïve Hb and MHb fail to increase ROS production in macrophages (Fig. 8D). Testing the effect of heme and the different Hb forms on macrophage viability revealed that heme at higher concentrations triggers cell death whereas Hb forms at the concentration of 250 µmol/L do not influence cell viability.

Taken together we demonstrated that following intravascular

hemolysis different Hb oxidation products are formed which might contribute to sterile hemolysis-induced inflammatory reactions. Among them, we identified FHb as a potent pro-inflammatory molecule that induces formation and maturation of the pro-inflammatory cytokine IL-1β *in vitro* and *in vivo*. FHb-mediated inflammatory response is mediated through NLRP3 inflammasome activation and caspase-1 activation. FHb acts as a heme source towards macrophages and increase ROS production. Further investigations are needed to identify the exact molecular mechanism of the pro-inflammatory actions of FHb. It needs to be addressed whether (i) FHb is internalized or (ii) the released heme exerts the biological effect of FHb or (iii) elevation of ROS production is involved in FHb-mediated pro-inflammatory responses in macrophages.

Accumulating evidence support the pathophysiological role of activation of the innate immune system in pathologies associated with intravascular hemolysis [20,21,23]. Thus, identification of RBC-derived DAMPs and understanding the molecular signaling mechanisms affected by them might provide new approaches for treating pathological conditions with intravascular lysis of RBCs.

Non-standard abbreviations

BMM	bone marrow-derived macrophage
CM-H_2DCFDA	5-(and-6)-chloromethyl-2′,7′-dichlorodihydro-fluorescein di-acetate acetyl ester
DAMPs	damage associated molecular patterns
DMEM	Dulbecco's Modified Eagle's Medium
FBS	fetal bovine serum
ferrylHb, FHb	ferryl hemoglobin
GAPDH	Glyceraldehyde 3-phosphate dehydrogenase
Hb	hemoglobin
Hct	hematocrit
HO-1	heme oxygenase-1
Hp	haptoglobin
Hx	hemopexin
IL-1β	interleukin 1 beta
LDL	low-density lipoprotein
LPS	lipopolysaccharide
MCV	mean corpuscular volume
metHb, MHb	methemoglobin
MTT	3-[4,5-Dimethylthiazol-2-yl]-2,5-diphenyl-tetrazolium bromide
NAC	*N*-acetyl cysteine
NLRP3	Nucleotide binding domain, Leucine rich Repeat containing Protein 3
PBS	phosphate buffered saline
PHZ	phenylhydrazine
RBCs	red blood cells
ROS	reactive oxygen species
TLR4	toll like receptor 4
TNF	tumor necrosis factor
WT	wild type

Acknowledgements

This work was supported by grant from the National Research, Development and Innovation Office (NKFIH grant number: K116024). The work was co-financed by the European Union and the European Social Fund under the GINOP-2.3.2-15-2016-00005 project.

Conflict of interest statement

The authors have no conflict of interest.

References

[1] M.A. Arruda, A.V. Graca-Souza, C. Barja-Fidalgo, Heme and innate immunity: new insights for an old molecule, Mem. Inst. Oswaldo Cruz 100 (7) (2005) 799–803.
[2] R. Mendonca, A.A. Silveira, N. Conran, Red cell DAMPs and inflammation, Inflamm. Res. 65 (9) (2016) 665–678.
[3] V. Jeney, et al., Natural history of the bruise: formation, elimination, and biological effects of oxidized hemoglobin, Oxidative Med. Cell. Longev. 2013 (2013) 703571.
[4] C.C. Winterbourn, Oxidative reactions of hemoglobin, Methods Enzymol. 186 (1990) 265–272.
[5] S. Harel, J. Kanner, The generation of ferryl or hydroxyl radicals during interaction of haemproteins with hydrogen peroxide, Free Radic. Res. Commun. 5 (1) (1988) 21–33.
[6] R.P. Patel, et al., Redox cycling of human methaemoglobin by H2O2 yields persistent ferryl iron and protein based radicals, Free Radic. Res. 25 (2) (1996) 117–123.
[7] Y. Jia, et al., Structural basis of peroxide-mediated changes in human hemoglobin: a novel oxidative pathway, J. Biol. Chem. 282 (7) (2007) 4894–4907.
[8] A.I. Alayash, R.P. Patel, R.E. Cashon, Redox reactions of hemoglobin and myoglobin: biological and toxicological implications, Antioxid. Redox Signal. 3 (2) (2001) 313–327.
[9] E. Nagy, et al., Oxidation of hemoglobin by lipid hydroperoxide associated with low-density lipoprotein (LDL) and increased cytotoxic effect by LDL oxidation in heme oxygenase-1 (HO-1) deficiency, Cell. Mol. Biol. (Noisy-le-Grand) 51 (4) (2005) 377–385.
[10] A.I. Alayash, Haptoglobin: Old protein with new functions. Clinica chimica acta, Int. J. Clin. Chem. 412 (7–8) (2011) 493–498.
[11] M. Kristiansen, et al., Identification of the haemoglobin scavenger receptor, Nature 409 (6817) (2001) 198–201.
[12] Z. Hrkal, Z. Vodrazka, I. Kalousek, Transfer of heme from ferrihemoglobin and ferrihemoglobin isolated chains to hemopexin, Eur. J. Biochem./FEBS 43 (1) (1974) 73–78.
[13] V. Hvidberg, et al., Identification of the receptor scavenging hemopexin-heme complexes, Blood 106 (7) (2005) 2572–2579.
[14] G. Balla, et al., Heme uptake by endothelium synergizes polymorphonuclear granulocyte-mediated damage, Trans. Assoc. Am. Phys. 103 (1990) 174–179.
[15] R. Gozzelino, M.P. Soares, Heme sensitization to TNF-mediated programmed cell death, Adv. Exp. Med. Biol. 691 (2011) 211–219.
[16] R. Gozzelino, V. Jeney, M.P. Soares, Mechanisms of cell protection by heme oxygenase-1, Annu. Rev. Pharmacol. Toxicol. 50 (2010) 323–354.
[17] V. Jeney, et al., Pro-oxidant and cytotoxic effects of circulating heme, Blood 100 (3) (2002) 879–887.
[18] M.P. Soares, M.T. Bozza, Red alert: labile heme is an alarmin, Curr. Opin. Immunol. 38 (2016) 94–100.
[19] R. Larsen, et al., Heme cytotoxicity and the pathogenesis of immune-mediated inflammatory diseases, Front. Pharmacol. 3 (2012) 77.
[20] R.T. Figueiredo, et al., Characterization of heme as activator of toll-like receptor 4, J. Biol. Chem. 282 (28) (2007) 20221–20229.
[21] J.D. Belcher, et al., Heme triggers TLR4 signaling leading to endothelial cell activation and vaso-occlusion in murine sickle cell disease, Blood 123 (3) (2014) 377–390.
[22] G. Chen, et al., Heme-induced neutrophil extracellular traps contribute to the pathogenesis of sickle cell disease, Blood 123 (24) (2014) 3818–3827.
[23] F.F. Dutra, et al., Hemolysis-induced lethality involves inflammasome activation by heme, Proc. Natl. Acad. Sci. U. S. A. 111 (39) (2014) E4110–E4118.
[24] J. Erdei, et al., Induction of NLRP3 inflammasome activation by heme in human endothelial cells, Oxidative Med. Cell. Longev. 2018 (2018) 4310816.
[25] N.S. Merle, et al., Intravascular hemolysis activates complement via cell-free heme and heme-loaded microvesicles, JCI Insight (2018) 3(12).
[26] M. Frimat, et al., Complement activation by heme as a secondary hit for atypical hemolytic uremic syndrome, Blood 122 (2) (2013) 282–292.
[27] N.S. Merle, et al., Characterization of renal injury and inflammation in an experimental model of intravascular hemolysis, Front. Immunol. 9 (2018) 179.
[28] C.B. Almeida, et al., Acute hemolytic vascular inflammatory processes are prevented by nitric oxide replacement or a single dose of hydroxyurea, Blood 126 (6) (2015) 711–720.
[29] G. Silva, et al., Oxidized hemoglobin is an endogenous proinflammatory agonist that targets vascular endothelial cells, J. Biol. Chem. 284 (43) (2009) 29582–29595.
[30] J. Balla, et al., Endothelial-cell heme uptake from heme proteins: induction of sensitization and desensitization to oxidant damage, Proc. Natl. Acad. Sci. U. S. A. 90 (20) (1993) 9285–9289.
[31] L. Potor, et al., Atherogenesis may involve the prooxidant and proinflammatory effects of ferryl hemoglobin, Oxidative Med. Cell. Longev. 2013 (2013) 676425.
[32] F. Martinon, et al., Gout-associated uric acid crystals activate the NALP3 inflammasome, Nature 440 (7081) (2006) 237–241.
[33] F.T. Meng, A.I. Alayash, Determination of extinction coefficients of human hemoglobin in various redox states, Anal. Biochem. 521 (2017) 11–19.
[34] M. Rosas, et al., The myeloid 7/4-antigen defines recently generated inflammatory macrophages and is synonymous with Ly-6B, J. Leukoc. Biol. 88 (1) (2010) 169–180.
[35] J. Gburek, et al., Hemoglobin - a novel ligand of hepatocyte ectopic F1-ATPase, J. Physiol. Pharmacol. 66 (6) (2015) 823–830.
[36] W.G. Siems, O. Sommerburg, T. Grune, Erythrocyte free radical and energy metabolism, Clin. Nephrol. 53 (1 Suppl) (2000) S9–17.
[37] V. Jeney, G. Balla, J. Balla, Red blood cell, hemoglobin and heme in the progression of atherosclerosis, Front. Physiol. 5 (2014) 379.
[38] B.J. Reeder, et al., Tyrosine as a redox-active center in electron transfer to ferryl heme in globins, Free Radic. Biol. Med. 44 (3) (2008) 274–283.

[39] L.J. Deterding, et al., Identification of free radicals on hemoglobin from its self-peroxidation using mass spectrometry and immuno-spin trapping: observation of a histidinyl radical, J. Biol. Chem. 279 (12) (2004) 11600–11607.
[40] D.C. Ramirez, Y.R. Chen, R.P. Mason, Immunochemical detection of hemoglobin-derived radicals formed by reaction with hydrogen peroxide: involvement of a protein-tyrosyl radical, Free Radic. Biol. Med. 34 (7) (2003) 830–839.
[41] E. Tolosano, et al., Enhanced splenomegaly and severe liver inflammation in haptoglobin/hemopexin double-null mice after acute hemolysis, Blood 100 (12) (2002) 4201–4208.
[42] Z. Gouveia, et al., Characterization of plasma labile heme in hemolytic conditions, FEBS J. 284 (19) (2017) 3278–3301.
[43] E.M. Welbourn, et al., The mechanism of formation, structure and physiological relevance of covalent hemoglobin attachment to the erythrocyte membrane, Free Radic. Biol. Med. 103 (2017) 95–106.
[44] K. Kuzelova, M. Mrhalova, Z. Hrkal, Kinetics of heme interaction with heme-binding proteins: the effect of heme aggregation state, Biochim. Biophys. Acta 1336 (3) (1997) 497–501.
[45] F. Vallelian, et al., Revisiting the putative role of heme as a trigger of inflammation, Pharmacol. Res. Perspect. 6 (2) (2018).
[46] S.M. Camus, et al., Circulating cell membrane microparticles transfer heme to endothelial cells and trigger vasoocclusions in sickle cell disease, Blood 125 (24) (2015) 3805–3814.
[47] C. Donadee, et al., Nitric oxide scavenging by red blood cell microparticles and cell-free hemoglobin as a mechanism for the red cell storage lesion, Circulation 124 (4) (2011) 465–U294.
[48] O. Rubin, et al., Red blood cell-derived microparticles isolated from blood units initiate and propagate thrombin generation, Transfusion 53 (8) (2013) 1744–1754.
[49] S.M. Camus, et al., Erythrocyte microparticles can induce kidney vaso-occlusions in a murine model of sickle cell disease, Blood 120 (25) (2012) 5050–5058.
[50] P.W. Buehler, et al., Haptoglobin preserves the CD163 hemoglobin scavenger pathway by shielding hemoglobin from peroxidative modification, Blood 113 (11) (2009) 2578–2586.
[51] S. Banerjee, et al., Haptoglobin alters oxygenation and oxidation of hemoglobin and decreases propagation of peroxide-induced oxidative reactions, Free Radic. Biol. Med. 53 (6) (2012) 1317–1326.
[52] Y.I. Miller, S.M. Altamentova, N. Shaklai, Oxidation of low-density lipoprotein by hemoglobin stems from a heme-initiated globin radical: antioxidant role of haptoglobin, Biochemistry 36 (40) (1997) 12189–12198.
[53] T. Pimenova, et al., Quantitative mass spectrometry defines an oxidative hotspot in hemoglobin that is specifically protected by haptoglobin, J. Proteome Res. 9 (8) (2010) 4061–4070.
[54] C.A. Schaer, et al., Mechanisms of haptoglobin protection against hemoglobin peroxidation triggered endothelial damage, Cell Death Differ. 20 (11) (2013) 1569–1579.
[55] C.B. Andersen, et al., Structure of the haptoglobin-haemoglobin complex, Nature 489 (7416) (2012) 456–459.
[56] J. Herz, D.K. Strickland, LRP: a multifunctional scavenger and signaling receptor, J. Clin. Invest. 108 (6) (2001) 779–784.
[57] D.J. Schaer, et al., Hemolysis and free hemoglobin revisited: exploring hemoglobin and hemin scavengers as a novel class of therapeutic proteins, Blood 121 (8) (2013) 1276–1284.
[58] D.J. Schaer, et al., Haptoglobin, hemopexin, and related defense pathways-basic science, clinical perspectives, and drug development, Front. Physiol. 5 (2014) 415.
[59] F.A.D.T.G. Wagener, et al., Heme is a potent inducer of inflammation in mice and is counteracted by heme oxygenase, Blood 98 (6) (2001) 1802–1811.
[60] B.N. Porto, et al., Heme induces neutrophil migration and reactive oxygen species generation through signaling pathways characteristic of chemotactic receptors, J. Biol. Chem. 282 (33) (2007) 24430–24436.
[61] R. Larsen, et al., A central role for free heme in the pathogenesis of severe sepsis, Sci. Transl. Med. 2 (51) (2010) 51ra71.
[62] A.P. Monteiro, et al., Leukotriene B4 mediates neutrophil migration induced by heme, J. Immunol. 186 (11) (2011) 6562–6567.
[63] E. Tolosano, et al., Enhanced splenomegaly and severe liver inflammation in haptoglobin/hemopexin double-null mice after acute hemolysis, Blood 100 (12) (2002) 4201–4208.
[64] A.N. Babu, et al., Hemoglobin-based oxygen carrier induces hepatic heme oxygenase 1 expression in Kupffer cells, Surgery 142 (2) (2007) 289–294.
[65] F. Alegre, P. Pelegrin, A.E. Feldstein, Inflammasomes in liver fibrosis, Semin. Liver Dis. 37 (2) (2017) 119–127.
[66] K. Schroder, J. Tschopp, The inflammasomes, Cell 140 (6) (2010) 821–832.
[67] G. Szabo, J. Petrasek, Inflammasome activation and function in liver disease, Nat. Rev. Gastroenterol. Hepatol. 12 (7) (2015) 387–400.
[68] G. Szabo, Gut-liver axis in alcoholic liver disease, Gastroenterology 148 (1) (2015) 30–36.
[69] J. Chavarria-Smith, R.E. Vance, The NLRP1 inflammasomes, Immunol. Rev. 265 (1) (2015) 22–34.
[70] E. Latz, T.S. Xiao, A. Stutz, Activation and regulation of the inflammasomes, Nat. Rev. Immunol. 13 (6) (2013) 397–411.
[71] J.A. Duncan, S.W. Canna, The NLRC4 inflammasome, Immunol. Rev. 281 (1) (2018) 115–123.
[72] J. Lugrin, F. Martinon, The AIM2 inflammasome: sensor of pathogens and cellular perturbations, Immunol. Rev. 281 (1) (2018) 99–114.
[73] Q.W. Li, et al., Heme induces IL-1 beta secretion through activating NLRP3 in kidney inflammation, Cell Biochem. Biophys. 69 (3) (2014) 495–502.
[74] M.P. Soares, R. Gozzelino, S. Weis, Tissue damage control in disease tolerance, Trends Immunol. 35 (10) (2014) 483–494.
[75] T. Kassa, et al., Differential heme release from various hemoglobin redox states and the upregulation of cellular heme oxygenase-1, FEBS Open Bio 6 (9) (2016) 876–884.
[76] J.M. Abais, et al., Redox regulation of NLRP3 inflammasomes: ROS as trigger or effector? Antioxid. Redox Signal. 22 (13) (2015) 1111–1129.
[77] R. Munoz-Planillo, et al., K(+) efflux is the common trigger of NLRP3 inflammasome activation by bacterial toxins and particulate matter, Immunity 38 (6) (2013) 1142–1153.
[78] C. Jin, R.A. Flavell, Molecular mechanism of NLRP3 inflammasome activation, J. Clin. Immunol. 30 (5) (2010) 628–631.
[79] V. Hornung, E. Latz, Critical functions of priming and lysosomal damage for NLRP3 activation, Eur. J. Immunol. 40 (3) (2010) 620–623.